THE EVOLUTION OF PLANETARY SYSTEMS WITH TIME-DEPENDENT STELLAR MASS LOSS RATES

Kassandra R. Anderson[1], Fred C. Adams[1,2], and Anthony M. Bloch[3]

[1]*Physics Department, University of Michigan, Ann Arbor, MI 48109*

[2]*Astronomy Department, University of Michigan, Ann Arbor, MI 48109*

[3]*Math Department, University of Michigan, Ann Arbor, MI 48109*

ABSTRACT

Observations indicate that intermediate mass stars, binary stars, and stellar remnants often host planets; a full explanation of these systems requires an understanding of how planetary orbits evolve as their central stars lose mass. Motivated by these dynamical systems, this paper generalizes previous studies of orbital evolution in planetary systems with stellar mass loss, with a focus on two issues: [1] Whereas most previous treatments consider constant mass loss rates, we consider single planet systems where the stellar mass loss rate is time dependent; the mass loss rate can be increasing or decreasing, but the stellar mass is always monotonically decreasing. We show that the qualitative behavior found previously for constant mass loss rates often occurs for this generalized case, and we find general conditions required for the planets to become unbound. However, for some mass loss functions, where the mass loss time scale increases faster than the orbital period, planets become unbound only in the asymptotic limit where the stellar mass vanishes. [2] We consider the chaotic evolution for two planet systems with stellar mass loss. Here we focus on a simple model consisting of analogs of Jupiter, Saturn, and the Sun. By monitoring the divergence of initially similar trajectories through time, we calculate the Lyapunov exponents of the system. This analog solar system is chaotic in the absence of mass loss with Lyapunov time $\tau_0 \approx 5$ Myr; we find that the Lyapunov time decreases with increasing stellar mass loss rate, with a nearly linear relationship between the two time scales. Taken together, results [1] and [2] help provide an explanation for a wide range of dynamical evolution that occurs in solar systems with stellar mass loss.

Subject headings: planets and satellites: dynamical evolution and stability — planet-star interactions — stars: evolution — stars: mass loss — white dwarfs

1. Introduction

Solar systems orbiting other stars display a diverse set of architectures and motivate further studies concerning the dynamics of planetary systems. Part of the richness of this dynamical problem arises from the intrinsic complexity of N-body systems, even in the absence of additional forces (Murray & Dermott 1999). The ledger of physical behavior experienced by such systems is enormous, and includes mean motion resonances, secular interactions, and sensitive dependence on the initial conditions (chaos). Additional complications arise from additional forces that are often present: During early stages of evolution, circumstellar disks provide torques that influence orbital elements, and turbulent fluctuations act on young planets. Over longer time scales, solar systems are affected by tidal forces from both stars and planets, and by general relativistic corrections that lead to orbital precession. Another classic problem in solar system dynamics concerns planetary orbits around central stars that are losing mass (Jeans 1924; see also Hadjidemetriou 1963, 1966). Although this issue has received some recent attention (see below), this paper expands upon existing work in two main directions. Most recent work focuses on the particular case of constant mass loss rates, although stellar mass loss typically varies with time. For single planet systems, we extend existing calculations to account for the time dependence of the mass loss. For systems with multiple (two) planets, we also show that the Lyapunov exponents, which determine the time scales for chaotic behavior, depend on the time scales for mass loss. As outlined below, these two results can account for a great deal of the possible behavior in solar systems where the central star loses mass.

A number of previous studies have considered planetary dynamics for host stars that are losing mass. For our own Solar System, long term integrations have been carried out to study the fate of the planets in light of mass loss from the dying Sun (Duncan & Lissauer 1998). Recent related work estimates an effective outer boundary r_B to the Solar System (due to stellar mass loss) in the range $r_B = 10^3 - 10^4$ AU, where orbiting bodies inside this scale remain safely bound (Veras & Wyatt 2012). Planets orbiting more massive stars, which lose a larger percentage of their mass, have their survival threatened by possible engulfment during the planetary nebula phase (Villaver & Livio 2007, Mustill & Villaver 2012), and are more likely to become unbound due to stellar mass loss alone (Villaver & Livio 2009). In the future of our own system, Earth is likely to be engulfed by the Sun (Schröder & Connon Smith 2008), but planets in wider orbits are expected to survive. However, gasoues planets that escape engulfment are still subject to evaporation and can experience significant mass loss (Bear & Soker 2011, Spiegel & Madhusudhan 2012). For planets orbiting stars that are losing mass, a more general treatment of the dynamics has been carried out for both single planet systems (Veras et al. 2011) and multiple planet systems (Veras & Tout 2012); these studies provide a comprehensive analysis for the particular case of constant mass loss rates. In

addition to causing planets to become unbound, stellar mass loss can drive orbital evolution that leads to unstable planetary systems surrounding the remnant white dwarfs remaining at the end of stellar evolution (Debes & Sigurdsson 2002). Indeed, observations indicate that white dwarfs can anchor both circumstellar disks (Melis et al. 2010) and planetary systems (Zuckerman et al. 2010); many white dwarf atmospheres contain an excess of heavy elements (Melis et al. 2010; Jura 2003), which is assumed to be a signature of accretion of a secondary body (a planet or asteroid). Finally, mass loss in binary star systems can lead to orbital instability, allowing planets to change their host star (Kratter & Perets 2012, Perets & Kratter 2012, Moeckel & Veras 2012).

This paper builds upon the results outlined above. Most previous studies have focused on cases where the stellar mass loss rates are constant in time. However, stars generally have multiple epochs of mass loss, and the corresponding rates are not constant. It is thus useful to obtain general results that apply to a wide class of mass loss functions. The first goal of this paper is to study single planet systems where the stellar mass loss rate varies with time. As the system loses mass, the semimajor axis of the orbit grows, and the planet becomes unbound for critical values of the stellar mass fraction ($m_f = M_f/M_0$). For systems that become unbound, we find the critical mass fraction m_f as a function of the mass loss rate and the form of the mass loss function. In other systems with mass loss, the orbit grows but does not become unbound. In these cases, we find the orbital elements at the end of the mass-loss epoch, again as a function of the mass loss rate and form of the mass loss function. For initially circular orbits and slow mass loss (time scales much longer than the initial orbital period), the critical mass fraction and/or the final orbital elements are simple functions of parameters that describe the mass loss rate. For initial orbits with nonzero eccentricity, however, the outcomes depend on the initial orbital phase. In this latter case, the allowed values of the critical mass fraction m_f (final orbital elements) take a range of values, which we estimate herein.

Next we consider multiple planet systems. If the planets are widely spaced, they evolve much like individual single planet systems. However, if the planets are sufficiently close together so that planet-planet interactions are important, the systems are generally chaotic. The second goal of this paper is thus to estimate the Lyapunov exponents for multiple-planet systems with stellar mass loss. For the sake of definiteness, we focus on two planet systems containing analogs of the Sun, Jupiter, and Saturn, i.e., bodies with the same masses and orbital elements. We find that the time scale for chaos (the inverse of the Lyapunov exponent) is proportional to the mass loss time scale. As a result, by the time the star has lost enough mass for the planets to become unbound, the planets have effectively erased their initial conditions (through chaos). For systems that evolve far enough in time, one can use the semi-analytic results derived for single planet systems with initially circular

orbits (see above) as a rough estimate of the conditions (e.g., the value of ξ_f) required for a planet to become unbound. Multiple planets and nonzero initial eccentricity act to create a distribution of possible values (e.g., for ξ_f) centered on these results. Since the systems are chaotic, and display sensitive dependence on initial conditions, one cannot unambiguously predict the value of ξ_f required for an planet to become unbound.

For completeness, we note that the problem of planetary orbits with stellar mass loss is analogous to the problem of planetary orbits with time variations in the gravitational constant G. For single planet systems (the pure two-body problem), the gravitational force depends only on the (single) product GM_*, so that the two problems are equivalent (e.g., Vinti 1974). However, for the case with time varying gravitational constant, the product GM_* could increase with time. Current experimental limits show that possible variations occur on time scales much longer than the current age of the universe (see the review of Uzan 2003), so that these effects only (possibly) become important in the future universe (Adams & Laughlin 1997). We also note that when considering time variations of the constants, one should use only dimensionless quantities, in this case the gravitational fine structure constant $\alpha_G = Gm_P^2/c\hbar$ (e.g., Duff et al. 2002).

This paper is organized as follows. We first present a general formulation of the problem of planetary orbits with stellar mass loss in Section 2 and then specialize to a class of models where the mass loss has a specific form (that given by equations [16] and [17]). These models include a wide range of behavior for the time dependence of the mass loss rates, including constant mass loss rate, exponential mass loss, and mass loss rates that decrease quickly with time, and these results are described in Section 3. In the following Section 4, we consider two planet systems and calculate the Lyapunov times scales for a representative sample of mass loss functions. The paper concludes, in Section 5, with a summary of our results and a discussion of their implications.

2. Model Equations for Orbits with Stellar Mass Loss

In this section we develop model equations for solar systems where the central star loses mass. We assume that mass loss takes place isotropically, so that the rotational symmetry of the system is preserved and the total angular momentum is a constant of motion. This constraint is explicitly satisfied in the analytical solutions that follow. For the numerical solutions, this property is used as a consistency check on the numerical scheme. On the other hand, the total energy of the system is not conserved because the total mass decreases with time (equivalently, the system no longer exhibits time reversal symmetry).

The general forms for the equations of motion with variable stellar mass are presented in many previous papers (from Jeans 1924 to Veras et al. 2011). Here we specialize to systems with a single planet and consider orbits with starting semimajor axis a. The specific angular momentum J, which is conserved, can be written in the form

$$J^2 = GM_0 a \, \eta \,, \tag{1}$$

where M_0 is the starting mass of the star. Equation (1) can be taken as the definition of the angular momentum parameter η. For a starting circular orbit, $\eta = 1$, whereas eccentric orbits have $\eta = 1 - e^2 < 1$, where e is the initial orbital eccentricity. The radial equation of motion can be written in the dimensionless form

$$\frac{d^2\xi}{dt^2} = \frac{\eta}{\xi^3} - \frac{m(t)}{\xi^2} \,, \tag{2}$$

where we have defined a dimensionless mass

$$m(t) \equiv \frac{M(t)}{M_0} \,. \tag{3}$$

We would like general solutions to the problem where the dimensionless mass of the star $m(t)$ is monotonically decreasing with time, but otherwise has an arbitrary time dependence. In the usual reduction of the two-body problem to an analogous one-body problem, the orbit described by the equation of motion is that of the reduced mass. In the dimensionless version of the problem with mass loss, represented by equation (2), the motion is also that of a reduced mass and the dimensionless stellar mass m is scaled (see Jeans 1924). In this treatment, we assume that mass loss takes place isotropically so that the reduced mass obeys equation (2), and the mass loss functions refer to the scaled stellar mass. In the limit where the planet mass M_P is small compared to the stellar mass M_*, scaling between the two-body problem and the equivalanet single body problem changes quantities by $\mathcal{O}(M_P/M_*)$.

In the dimensionless problem, the starting semimajor axis is unity (by definition) and the initial conditions require that the starting radial coordinate ξ_0 lies in the range $1 - e \le \xi_0 \le 1 + e$, where the starting eccentricity e is given by $\eta = 1 - e^2$. The initial energy $\mathcal{E}_0 = -1/2$ in these units and the initial velocity $\dot{\xi}_0$ is given by

$$\dot{\xi}_0^2 = \frac{2\xi_0 - \eta - \xi_0^2}{\xi_0^2} = \frac{[(1 + e) - \xi_0][\xi_0 - (1 - e)]}{\xi_0^2} \,. \tag{4}$$

The initial velocity can be positive or negative, where the sign depends on the starting phase of the orbit.

2.1. Change of Variables

The equation of motion (2) is complicated because it contains an arbitrary function, namely $m(t)$, that describes the mass loss history. On the other hand, the independent variable (time) does not appear explicitly. As a result, we define a new effective "time" variable u through the expression

$$u \equiv \frac{1}{m} \,, \tag{5}$$

where $m = m(t)$. The generalized time variable u starts at $u = 1$ and is monotonically increasing. In terms of the variable u, the basic equation of motion (2) takes the form

$$\dot{u}^2 \frac{d^2\xi}{du^2} + \ddot{u}\frac{d\xi}{du} = \frac{\eta}{\xi^3} - \frac{1}{u\xi^2} \,. \tag{6}$$

Next we note that both standard lore and numerical solutions (beginning with Jeans 1924) show that, in physical units, the product $aM \approx constant$. In terms of the current dimensionless variables, this finding implies that the function

$$f \equiv \frac{\xi}{u} = \xi m \tag{7}$$

should vary over a limited range. We thus change the dependent variable from ξ to f and write the equation of motion in the form

$$\dot{u}^2 u^2 f^3 \left[\left(u^2 f'' + 2uf' \right) + \frac{u\ddot{u}}{\dot{u}^2} \left(uf' + f \right) \right] = \eta - f \,, \tag{8}$$

where primes denote derivatives with respect to the variable u. Note that the time scale for mass loss is given by $u/\dot{u}$ and that the orbital time scale (the inverse of the orbital frequency) is given by $u^2 f^{3/2}$ (keep in mind that the inverse orbital frequency is shorter than the orbital period by a factor of 2π). The ratio λ of these two fundamental time scales is given by

$$\lambda^2 \equiv \dot{u}^2 u^2 f^3 \,. \tag{9}$$

The leading coefficient in equation (8) is thus λ^2, the square of the ratio of the orbital time scale to the time scale for mass loss. For small values of λ^2, the mass loss time is long compared to the orbit time, and the orbits are expected to be nearly Keplerian; for larger λ^2, the star loses mass a significant amount of mass per orbit and a Keplerian description is no longer valid. For the former case, where mass loss is slow compared to the orbit time, we can use the parameter λ to order the terms in our analytic estimates.

In addition to the coefficient λ^2, given by the ratio of time scales, another important feature of equation (8) is the index β appearing within the square brackets, where

$$\beta \equiv \frac{u\ddot{u}}{\dot{u}^2} \,. \tag{10}$$

The index β encapsulates the time dependence of the mass loss (see Section 2.3).

2.2. Orbital Energy

For the chosen set of dimensionless variables, the energy $\mathcal{E}$ of the system takes the form

$$\mathcal{E} = \frac{1}{2}\dot{u}^2 \left(uf' + f\right)^2 + \frac{\eta}{2u^2 f^2} - \frac{1}{u^2 f} . \tag{11}$$

The energy has a starting value $\mathcal{E} = -1/2$, by definition, and increases as mass loss proceeds. If and when the energy becomes positive, the planet is unbound. Although the energy expression (11) appears somewhat complicated, the time dependence of the energy reduces to the simple form

$$\frac{d\mathcal{E}}{du} = \frac{1}{u^3 f} . \tag{12}$$

Note that the derivative of the energy is positive definite, so that the energy always increases. Since the energy is negative and strictly increasing, the semimajor axis of the orbit, when defined according to $a \propto |\mathcal{E}|^{-1}$, is also monotonically increasing.

It is useful to consider some simple cases for illustration: If the function f is constant, then the energy can be integrated to obtain the form

$$\mathcal{E}(u) = -\frac{1}{2} + \frac{1}{2f}\left(1 - \frac{1}{u^2}\right) . \tag{13}$$

In this case, if $f = 1$, the energy only become positive in the limit $u \to \infty$, which corresponds to the star losing all of its mass. If the function $f < 1$, but still constant, the system becomes unbound when

$$u = (1 - f)^{-1/2} \to \frac{1}{e} . \tag{14}$$

To obtain the second limiting form, we assume that $f = \eta = 1 - e^2$, where e is the starting orbital eccentricity (which remains constant in this example).

In the regime of $\lambda \gg 1$ and large u, the solutions often have the form $f \sim 1/u$. In this case, we can integrate the energy from the point where this form of the solution becomes valid. Here we redefine the variables so that $\xi = 1$ and $u = 1$ at this transition point, and hence the energy $\mathcal{E}_0 = -1/2$ and $f = 1/u$. The energy thus has the simple form

$$\mathcal{E} = -\frac{1}{2} + \left(1 - \frac{1}{u}\right) = \frac{1}{2} - \frac{1}{u} . \tag{15}$$

In this case, the energy becomes positive when the star loses half of its half ($m = 1/2$ or $u = 2$) as expected.

2.3. Mass Loss Functions

Next we want to specialize to the specific where $\beta = constant$, which represents a class of mass loss functions. In this case, the defining equation (10) for the mass loss index can be integrated to obtain the form

$$\dot{u} = \gamma u^\beta \,, \tag{16}$$

where γ is a constant that defines the mass loss rate at the beginning of the epoch (when $t = 0$, $m = 1$, and $u = 1$). For a given (constant) value of the index β, the dimensionless mass loss rate has the form

$$\dot{m} = -\gamma m^{(2-\beta)} \,. \tag{17}$$

In addition to simplifying the equation of motion, this form for the mass loss function is motivated by stellar behavior, as discussed below.

The mass loss rate of stars is often characterized by the physically motivated form

$$\dot{M} = -\dot{M}_0 \left(\frac{L_*}{L_\odot} \right) \left(\frac{R_*}{R_\odot} \right) \left(\frac{M_*}{M_\odot} \right)^{-1} \,, \tag{18}$$

where $\dot{M}_0$ is constant and depends on the phase of stellar evolution under consideration (Kudritzki & Reimers 1978, Hurley et al. 2000). Since the radius and luminosity depend on stellar mass (for a given metallicity), the physically motivated expression of equation (18) can take the same form as the model from equation (17), which corresponds to a constant mass loss index (see equations [10] and [16]).

Using the scaling law (18), the power-law index appearing in equation (17) can be positive or negative, depending on how the stellar luminosity and radius vary with mass during the different phases of mass loss (see Hurley et al. 2000 for a detailed discussion). For example, if we consider main-sequence stars, the stellar cores adjust quickly enough that the luminsoity obeys the standard mass-luminosity relationship $L_* \sim M_*^p$ (where the index $p \approx 3$) and the mass-radius relationship $R_* \sim M_*^q$ (where the index q typically falls in the range $1/2 \leq q \leq 1$). For main-sequence stars we thus obtain the scaling law $\dot{m} \sim -m_m^\alpha$, where the index $\alpha_m = p+q-1$ is predicted to lie in the range $2.5 \leq \alpha_m \leq 3$; the corresponding mass loss index lies in the range $-1 \leq \beta \leq -1/2$. Next we consider stars on the first giant branch or the asymptotic giant branch. In this phase of stellar evolution, mass loss occurs from an extended stellar envelope, but the luminosity is produced deep within the stellar core. As the star loses mass, the core and hence the luminosity remains relatively constant, whereas the radius scales approximately as $R_* \sim M_*^{-1/3}$ (Hurley et al. 2000). For this case, one obtains the scaling law $\dot{m} \sim -m^{-4/3}$, with an mass loss index $\beta = 10/3$. In general, for $\dot{m} \sim -m_m^\alpha$, the mass loss index $\beta = 2 - \alpha_m$. As these examples show, the mass loss index can take on a wide range of values $-1 \leq \beta \leq 4$.

To fix ideas, we consider the time dependence for mass loss functions that are often used. For a constant mass loss rate, the most common assumption in the literature, the index $\beta = 2$, and the mass evolution function has the form

$$m(t) = 1 - \gamma t \qquad \text{and} \qquad u(t) = \frac{1}{1 - \gamma t} \,. \tag{19}$$

The value $\beta = 2$ marks the boundary between models where the mass loss rate accelerates with time ($\beta > 2$) and those that decelerate ($\beta < 2$). For the case of exponential time dependence of the stellar mass, the index $\beta = 1$, and the mass loss function has the form

$$m(t) = \exp[-\gamma t] \qquad \text{and} \qquad u(t) = \exp[\gamma t] \,. \tag{20}$$

The value $\beta = 1$ marks the boundary between models where the system reaches zero stellar mass in a finite time ($\beta > 1$), and those for which the mass $m \to 0$ only in the limit $u \to \infty$. For the case with index $\beta = 0$, which represents an important test case, the mass evolution function becomes

$$m(t) = \frac{1}{1 + \gamma t} \qquad \text{and} \qquad u(t) = 1 + \gamma t \,. \tag{21}$$

For $\beta = 0$, analytic solutions are available (see Section 3.2), which inform approximate treatments for more general values of the index β. Finally, the case where $\beta = -1$ plays a defining role (see Section 3.1) and corresponds to the forms

$$m(t) = (1 + 2\gamma t)^{-1/2} \qquad \text{and} \qquad u(t) = (1 + 2\gamma t)^{1/2} \,. \tag{22}$$

The value $\beta - 1$ marks the boundary between models where the planet becomes unbound at finite stellar mass ($\beta > -1$) and those for which the planet becomes unbound only in the limit $m \to 0$ or $u \to \infty$ ($\beta < -1$). In general, for constant $\beta \neq 1$, the time dependence of the mass takes the form

$$m(t) = \frac{1}{u(t)} = [1 - (\beta - 1)\gamma t]^{1/(\beta - 1)} \,. \tag{23}$$

The particular case $\beta = 1$ results in the decaying exponential law of equation (20).

2.4. Equation of Motion with Constant Mass Loss Index

For constant values of the mass loss index β, the equation of motion reduces to the form

$$\lambda^2 \left[u^2 f'' + (2 + \beta)u f' + \beta f \right] = \eta - f \,, \tag{24}$$

where the ratio of time scales λ is given by

$$\lambda^2 = \gamma^2 u^{2\beta + 2} f^3 \,. \tag{25}$$

By writing the equation of motion in the form (24), we immediately see several key features of the solutions:

When the parameter $\lambda \ll 1$, the left-hand side of equation (24) is negligible, and the equation of motion reduces to the approximate form $f \approx \eta = constant$. This equality is only approximate, because the function f also executes small oscillations about its mean value as the orbit traces through its nearly elliptical path (see below). Nonetheless, this behavior is often seen in numerical studies of planetary systems with stellar mass loss (e.g., Veras et al. 2010; see also Debes & Sigurdsson 2002). The form of equation (24) makes this behavior clear. Note that this regime is sometimes called the "adiabatic regime"; however, this terminology is misleading, because "adiabatic" refers to evolution of a thermodynamic system at constant energy (heat), whereas the systems in question steadily lose energy through stellar mass loss.

When the parameter $\lambda \gg 1$, the left-hand side of equation (24) dominates, the solutions for $f(u)$ take the form of power-laws with negative indices. In this limit, the equation of motion approaches the approximate form

$$u^2 f'' + (2 + \beta)uf' + \beta f = 0 \,.\tag{26}$$

In this regime, the function f has power-law solutions with indices p given by the quadratic equation

$$(p + 1)(p + \beta) = 0 \,.\tag{27}$$

The general form for the solution $f(u)$ in this regime is thus

$$f(u) = \frac{A}{u} + \frac{B}{u^\beta} \,.\tag{28}$$

Once the solutions enter into the power-law regime, the energy can quickly grow and the planet can become unbound. To illustrate this behavior, consider the differential equation (12) for the orbital energy. We first consider the regime where $\lambda \ll 1$ and the function f is nearly constant. For the benchmark case $f = 1$, the equation can be integrated to obtain

$$\mathcal{E} = -\frac{1}{2u^2} \,.\tag{29}$$

Thus, as long as $f = 1$, the energy remains negative and the planet remains bound, except in the limit $u \to \infty$. Now consider the case where $\lambda > 1$ and the solutions enter into the power-law regime. If we now consider the case $f = A/u$, for example, the differential equation for energy can be integrated to obtain

$$\mathcal{E} = \mathcal{E}_x + \frac{1}{Au_x} \left(1 - \frac{u_x}{u}\right) \,,\tag{30}$$

where the subscript x denotes a reference point where the solutions enters into the power-law regime. Since $Au_x < 1$ and $|\mathcal{E}_x| < 1/2$, the energy quickly becomes positive once the power-law regime is reached.

In order for the solution to make the transition from $f \approx constant$ to the power-law solutions that cause the orbits to become unbound, the ratio of time scales λ must grow with time. However, growth requires that $\beta > -1$ (see equation [25]). We can understand this requirement as follows: The orbital time scale P varies with u (and hence time) according to $P \sim u^2 f^{3/2}$. Since f is nearly constant, this relation simplifies to the form $P \sim u^2$. The time scale for mass loss τ is given by $\tau = u/\dot{u}$, which has the form $\tau \sim u^{1-\beta}$ from equation (16). As a result, when $\beta = -1$, the orbit time has the same dependence on stellar mass as the mass loss time scale, so that the ratio λ is nearly constant as the star loses mass. For $\beta < -1$, the ratio λ of time scales decreases with time, and the system grows "more stable".

3. Results for Single Planet Systems with Stellar Mass Loss

This section presents the main results of this paper for single planet systems with a central star that loses mass. We first consider three special cases: First, we consider mass loss index $\beta = -1$, which marks the critical value such that systems with $\beta > -1$ become unbound at finite values of the stellar mass, whereas systems with $\beta < -1$ only become unbound in the limit $m \to 0$. Next we consider mass loss index $\beta = 0$; in this case, the solutions can be found analytically, and these results guide an approximate analytic treatment of the general case. We also consider the limiting case where stellar mass loss takes place rapidly.

3.1. The Transition Case

Here we consider the case where the mass loss index $\beta = -1$, which corresponds to the transition value between cases where the ratio λ of time scales grows with time $(\beta > -1)$ and those where the ratio decreases with time $(\beta < -1)$. In this regime, the equation of motion reduces to the form

$$\gamma^2 \left[u^2 f'' + u f' - f \right] = \frac{\eta}{f^3} - \frac{1}{f^2} \,. \tag{31}$$

The equation of motion can be simplified further by making the change of (independent) variable

$$w \equiv \log u \,, \tag{32}$$

so that the equation of motion becomes

$$\gamma^2 \left[\frac{d^2 f}{dw^2} - f \right] = \frac{\eta}{f^3} - \frac{1}{f^2} \,. \tag{33}$$

This version of the equation of motion (first considered by Jeans 1924) contains no explicit dependence on the independent variable w, so that the equation can be integrated to obtain the expression

$$\gamma^2 \left(\frac{df}{dw} \right)^2 = \gamma^2 f^2 + \frac{2}{f} - \frac{\eta}{f^2} - E \,, \tag{34}$$

where E is a constant that plays the role of energy. Note that we have chosen the sign such that $E > 0$ and that $E = 1$ for initially circular orbits. In order for the function $f(w)$ to have oscillatory solutions, the fourth order polynomial

$$p(f) = \gamma^2 f^4 - E f^2 + 2f - \eta \tag{35}$$

must be positive between two positive values of f. In order for this requirement to be met, the parameters must satisfy the inequalities

$$\eta E \leq \frac{9}{8} \qquad \text{and} \qquad \gamma \leq (E/3)^{3/4} \,. \tag{36}$$

The first inequality is always satisfied for the cases of interest. The second inequality in equation (36) determines the maximum value of the mass loss parameter γ for which oscillatory solutions occur.

3.2.   Systems with Vanishing Mass Loss Index

In the particular case where $\beta = 0$, the equation of motion can be simplified. In particular the first integral can be taken analytically to obtain the form

$$\gamma^2 \left(u^2 f' \right)^2 = -\frac{\eta}{f^2} + \frac{2}{f} - E \,. \tag{37}$$

The constant of integration E is essentially the energy of the orbit. Since energy is negative for a bound orbit, the choice of sign makes $E > 0$. The factor of 2 in the definition is for convenience. The value of E depends on the initial configuration. For the particular case where the orbit starts at periastron, for example, the initial speed $\dot{\xi} = 0$ and the energy constant has the value

$$E = 1 - \gamma^2 (1 - e)^2 \,, \tag{38}$$

where the eccentricity $e = (1 - \eta)^{1/2}$. In general, the initial value $f_0 = \xi_0$ can lie anywhere in the range $1 - e \leq f_0 \leq 1 + e$, and the energy constant has the general form

$$E = 1 - \gamma^2 f_0^2 \pm 2\gamma \left[2f_0 - \eta - f_0^2\right]^{1/2} , \qquad (39)$$

where the choice of sign is determined by whether the planet is initially moving outward $(+)$ or inward $(-)$. With the energy constant E specified, the turning points for the function f are found to be

$$f_{1,2} = \frac{1 \pm [1 - \eta E]^{1/2}}{E} . \qquad (40)$$

If we consider the function f to play the role of the radial coordinate, then equation (40) defines analogs of the semimajor axis a_* and eccentricity e_*, which are given by

$$a_* = \frac{1}{E} \qquad \text{and} \qquad e_* = [1 - \eta E]^{1/2} . \qquad (41)$$

For the particular case where the orbit starts at periastron, the effective eccentricity has the form

$$e_* = \left[e^2 + \gamma^2(1 - e)^3(1 + e)\right]^{1/2} , \qquad (42)$$

whereas the for the general case

$$e_* = \left[e^2 + \gamma^2(1 - e^2)f_0^2 \mp 2\gamma(1 - e^2)\left(2f_0 - \eta - f_0^2\right)^{1/2}\right]^{1/2} . \qquad (43)$$

Note that the effective eccentricity e_* of the function f is larger than the initial eccentricity e of the original orbit (before the epoch of mass loss). In particular, for a starting circular orbit $e = 0$, the effective eccentricity $e_* = \gamma \neq 0$. The integrated equation of motion (37) can then be separated and written in the form

$$\frac{f\,df}{[(f - f_1)(f_2 - f)]^{1/2}} = \frac{E^{1/2}}{\gamma}\frac{du}{u^2} . \qquad (44)$$

If we integrate this equation from one turning point to the other, the change in mass of the system the same for every cycle, i.e.,

$$\Delta m = \frac{\gamma\pi}{E^{3/2}} , \qquad (45)$$

where E is given by equation (39). Following standard procedures, we can find the solution for the orbit shape, which can be written in the from

$$\frac{\eta}{f} = \frac{\eta\,u}{\xi} = 1 + e_*\cos\theta . \qquad (46)$$

The orbit equation thus takes the usual form, except that the original eccentricity e is replaced with the effective eccentricity e_* and the effective "radius" variable (f) scales with the mass/time variable $u = 1/m$.

For this mass loss function (with $\beta = 0$), we can find a simple relationship between the value of the time scale ratio λ and the value of f when the planet becomes unbound. To obtain this result, we insert the first integral from equation (37) into the general expression (11) for the energy $\mathcal{E}$ of the orbit and set $\mathcal{E} = 0$. After eliminating the derivative f', we can solve for the time scale ratio λ_f as a function of the final value of f. When the planet becomes unbound, the time scale ratio is thus given by

$$\lambda_f = \frac{(2f - \eta)^{1/2} \pm (2f - \eta - f^2)^{1/2}}{f^{1/2}}. \tag{47}$$

Here, f is the evaluated when the planet become unbound. In this case, however, the value of f is constrained to lie in the range $f_1 \leq f \leq f_2$, where the turning points are given by equation (40). For small γ, the orbit oscillates back and forth between the turning points many times before the planet becomes unbound. The final value of f is thus an extremely sensitive function of the starting orbital phase. This extreme sensitivity is not due to chaos, and can be calculated if one knows the exact orbital phase at the start. In practice, however, the final value of f can be anywhere in the range $f_1 \leq f \leq f_2$.

Figure 1 shows the final values of the time scale ratio λ as a function of the final value of $f = \xi/u = \xi m$. Curves are shown for nine values of the starting eccentricity, where $e = 0.1, 0.2, \ldots 0.9$. The innermost (outermost) closed curve in the figure corresponds to the smallest (largest) eccentricity. Each value of f corresponds to two possible values of the time scale ratio λ, one for orbits that are increasing in f and one for orbits that are decreasing in f at the time when the planet becomes unbound. These two values of λ (for a given f) correspond to the two branches of the solution given by equation (47).

For comparison, Figure 2 shows the same plane of parameters for the final values of the time scale ratio λ_f and f_f for planetary systems with constant mass loss rate (where $\beta = 2$). Note that the range of allowed values for the time scale ratio λ_f is much larger than for the case with $\beta = 0$, whereas the range of final values f_f is somewhat smaller.

One can also show that for circular orbits ($\eta = 1$ and $e = 0$), the value of the time scale ratio $\lambda = 1$ when the planet becomes unbound. For circular orbits in the limit $\gamma \to 0$, the turning points of the orbit approach $f_{1,2} = 1$. Using $f = 1$ and $\eta = 1$ in equation (47), we find $\lambda = 1$.
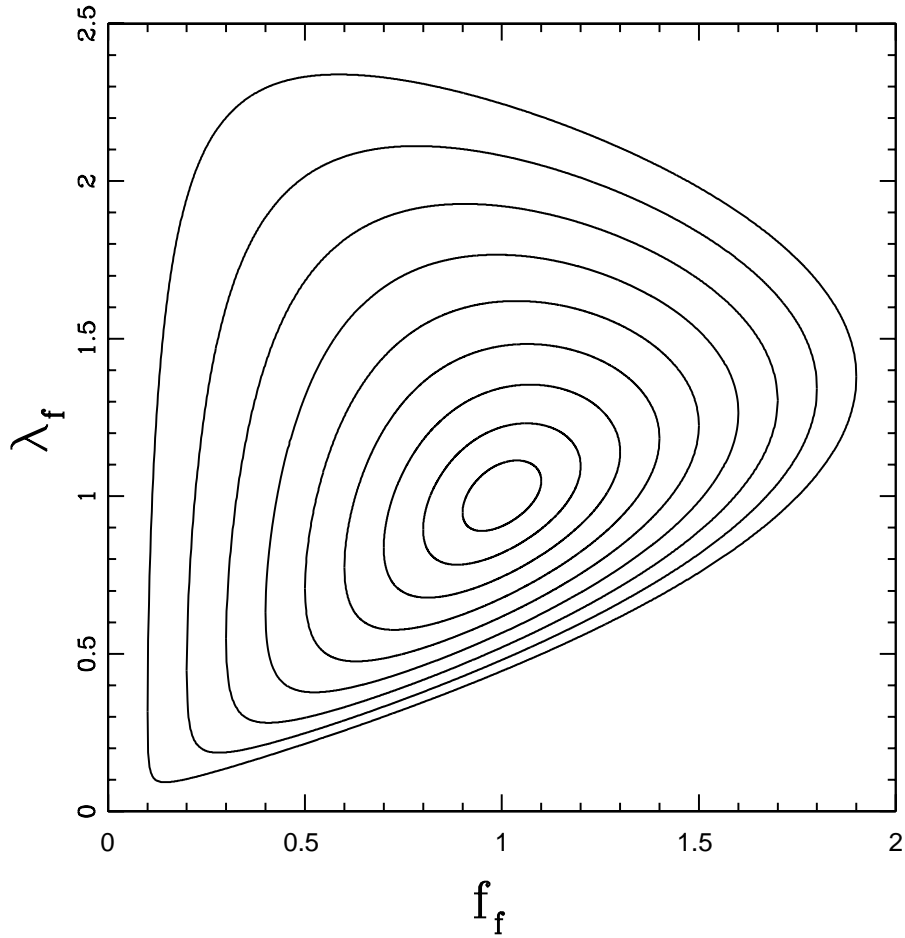
Fig. 1.— Time scale ratio λ_f as a function of the final value of $f = f_f$ for planetary systems with $\beta = 0$. For a given angular momentum η, specified by the starting eccentricity, the allowed values of λ_f form closed curves in the plane as shown. Curves are shown for a range of starting eccentricity, from $e = 0.1$ (inner curve) to $e = 0.9$ (outer curve).
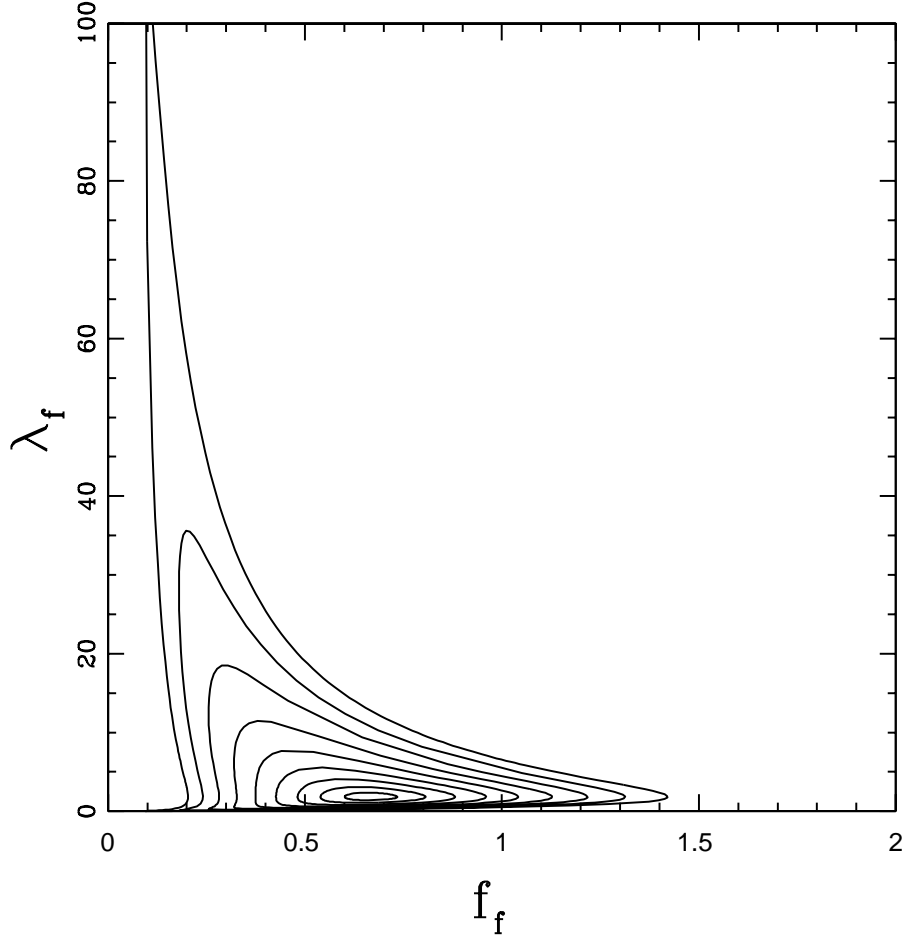
Fig. 2.— Time scale ratio λ_f as a function of the final value of $f = f_f$ for planetary systems with $\beta = 2$ (constant mass loss rates). For a given angular momentum η, specified by the starting eccentricity, the allowed values of λ_f form closed curves in the plane as shown. Curves are shown for a range of starting eccentricity, from $e = 0.1$ (inner curve) to $e = 0.9$ (outer curve). Compare with Figure 1 (and note the change of scale).

3.3. Limit of Rapid Mass Loss

If we now consider the case where the mass loss is rapid, so that the equation of motion has solution (28) throughout the evolution, we can fix the constants A and B by applying the initial conditions. Since $f = \xi/u$ and $u = 1$ at the start of the epoch, $f(1) = \xi_1$, where ξ_1 is the starting value of the orbital radius. By definition, the semimajor axis is unity, and the starting orbital eccentricity is given $e^2 = 1 - \eta$. The starting radius thus lies in the range

$$1 - \sqrt{1 - \eta} \leq \xi_1 \leq 1 + \sqrt{1 - \eta} \,, \tag{48}$$

which is equivalent to $1 - e \leq \xi_1 \leq 1 + e$. The derivative f' is given by

$$f' = \frac{df}{du} = -\frac{\xi}{u^2} + \frac{\xi'}{u} = -\frac{\xi}{u^2} + \frac{1}{u\dot{u}}\frac{d\xi}{dt} = -\frac{\xi}{u^2} + \frac{1}{\gamma u^{\beta+1}}\frac{d\xi}{dt} \,. \tag{49}$$

In the regime of interest where $\gamma \gg 1$, the second term is small compared to the first. In this limit, $f'(1) = -\xi_1$, where ξ_1 lies in the range indicated by equation (48). The constants A and B are thus determined to be $B = 0$ and $A = \xi_1$, so that the solution has the simple form

$$f(u) = \frac{\xi_1}{u} \,. \tag{50}$$

The energy of the orbit, by definition, starts at $\mathcal{E}(u = 1) = \mathcal{E}_1 = -1/2$, and the energy obeys the differential equation (12). Combining the solution of equation (50) with the differential equation (12) for energy, we can integrate to find the energy as a function of u (equivalent to time or mass),

$$\mathcal{E} = -\frac{1}{2} + \frac{1}{\xi_1}\left(1 - \frac{1}{u}\right) \,. \tag{51}$$

We can then read off the value of u_*, and hence the mass m_*, where the energy becomes positive and the planet becomes unbound, i.e.,

$$m_* = \frac{1}{u_*} = 1 - \frac{\xi_1}{2} \,. \tag{52}$$

Note that this critical value of the mass depends on the orbital phase of the planet within its orbit (i.e., the result depends on ξ_1 rather than the starting semimajor axis, which is unity).

For cases where the mass loss is rapid, but the planet remains bound, we can find the orbital properties for the post-mass-loss system. Consider the limiting case where the star has initial mass $m = 1$, and loses a fraction of its mass instantly so that it has a final mass m_∞, i.e.,

$$m(t) = m_\infty + (1 - m_\infty)H(-t) \,, \tag{53}$$

where H is the Heaviside step function. The mass loss thus occurs instantaneously at $t = 0$. For $t < 0$, the solutions to the orbit equation (2) have the usual form,

$$\dot{\xi}^2 = \frac{2}{\xi} - \frac{\eta}{\xi^2} - 1 = \frac{(\xi - \xi_1)(\xi_2 - \xi)}{\xi^2}, \tag{54}$$

where $\xi_{2,1} = 1 \pm e$ and $\eta = 1 - e^2$. After mass loss has taken place, the new (dimensionless) stellar mass is m_∞, and the first integral of the equation of motion can be written in the form

$$\dot{\xi}^2 = \frac{2m_\infty}{\xi} - \frac{\eta}{\xi^2} - 1 + \frac{2(1 - m_\infty)}{\xi_0}, \tag{55}$$

where the final constant term takes into account the change in (dimensionless) energy at the moment of mass loss. The radial position at $t = 0$ is ξ_0; since the planet is initially in a bound elliptical orbit, the radial coordinate must lie in the range $1 - e \leq \xi_0 \leq 1 + e$. The energy $\mathcal{E}$ of the new orbit is thus given by

$$2\mathcal{E} = -1 + \frac{2(1 - m_\infty)}{\xi_0}. \tag{56}$$

The energy $\mathcal{E}$ is negative, and the orbit is bound, provided that the remaining mass $m_\infty > 1 - \xi_0/2$. This condition is thus consistent with equation (52), which defines the mass scale at which orbits become unbound in the limit of rapid mass loss. In terms of the energy $\mathcal{E}$, the turning points of the new orbit take the form

$$\xi_\pm = \frac{m_\infty \pm [m_\infty^2 - 2|\mathcal{E}|\eta]^{1/2}}{2|\mathcal{E}|}. \tag{57}$$

We can then read off the orbital elements for the new (post-mass-loss) orbit, i.e.,

$$a = \frac{m_\infty}{2|\mathcal{E}|} \quad \text{and} \quad e = \sqrt{1 - 2|\mathcal{E}|\eta/m_\infty^2}, \tag{58}$$

where the new orbital energy $\mathcal{E}$ is given by equation (56).

3.4. Analytic Results for General Mass Loss Indices

In order to address the general case, we first change variables according to the ansatz

$$x = u^\alpha \quad \text{where} \quad \alpha = \beta + 1. \tag{59}$$

After substitution, the equation of motion becomes

$$\gamma^2 \alpha^2 x^2 \left[x^2 f_{xx} + 2x f_x \right] + \gamma^2 \beta x^2 f = \frac{\eta}{f^3} - \frac{1}{f^2}, \tag{60}$$

where the subscripts denote derivatives with respect to the new variable x. The ratio of time scales is now given by

$$\lambda^2 = \gamma^2 x^2 f^3 . \tag{61}$$

In general, we can write the first integral in the implicit form

$$\gamma^2 \alpha^2 \left[x^2 f_x \right]^2 + 2\gamma^2 \beta \int_1^x x^2 f f_x dx = -\frac{\eta}{f^2} + \frac{2}{f} - E , \tag{62}$$

where $E > 0$ has the same meaning as before. To move forward, we can define

$$J \equiv 2\gamma^2 \beta \int_1^x x^2 f f_x dx, , \tag{63}$$

so that

$$\gamma^2 \alpha^2 \left[x^2 f_x \right]^2 + J = \frac{2f - \eta - E f^2}{f^2} . \tag{64}$$

Note that $J = \mathcal{O}(\lambda^2)$, which means that J will be negligible for most of the evolution (see Appendix A). The energy of the system can be written in the form

$$u^2 \mathcal{E} = \frac{1}{2} \gamma^2 x^2 (\alpha x f_x + f)^2 + \frac{\eta}{2f^2} - \frac{1}{f} . \tag{65}$$

At the start of the evolution (where $u = 1$ and $x = 1$), the energy $\mathcal{E} = -1/2$ by definition. Using this specification, we can find the value of the integration constant E, which takes the form

$$E = 1 - \gamma^2 f_0^2 \pm 2\gamma \left(2f_0 - \eta - f_0^2 \right)^{1/2} , \tag{66}$$

where $f_0 (= \xi_0)$ is the starting value of the function (radial variable).

At an arbitrary time during the epoch of mass loss, we can write the derivative f_x in the form

$$\gamma \alpha \left[x^2 f_x \right] = \pm \left(\frac{2f - \eta - E f^2}{f^2} - J \right)^{1/2} = \pm \frac{1}{f} \left(2f - \eta - E f^2 - J f^2 \right)^{1/2} . \tag{67}$$

Since $J = \mathcal{O}(\lambda^2)$, $|J| \ll E$ for most of the evolution. As a result, working to leading order, we can set $J = 0$ in equation (67) and recover the same orbital solutions found earlier in Section 3.2. The only difference is that the dependent (time) variable u is replaced with $x = u^{\beta+1}$. As a result, the turning points for the function $f(x)$ will be given by equation (40) and the orbital elements for $f(x)$ are given by equation (41).

The basic behavior of the orbit is illustrated by Figure 3. The function f, plotted here versus u as the solid black curve, oscillates between the turning points (marked by the red horizontal lines) given by equation (40). The radial coordinate (here $\log \xi$ is plotted as the

dotted blue curve) oscillates also, but grows steadily. The eccentricity of the orbit (green dashed curve) also oscillates, but grows with time. Finally, the time scale ratio λ (magenta dot-dashed curve) also oscillates and grows with time. The simple oscillatory behavior for $f(u)$ ceases near the point where the time scale ratio λ becomes of order unity. Note that the function f falls outside the boundary marked by the turning points near $u = 12$ in the Figure.

Next we consider the time evolution of the energy of the orbit. After some rearrangement, the energy from equation (65) can be rewritten in the form

$$2u^2 \mathcal{E} = -E - J \pm 2\gamma x \left(2f - \eta - Ef^2 - Jf^2\right)^{1/2} + \gamma^2 x^2 f^2, \tag{68}$$

or, to leading order,

$$2u^2 \mathcal{E} = -E \pm 2\gamma x \left(2f - \eta - Ef^2\right)^{1/2} + \mathcal{O}\left(\lambda^2\right). \tag{69}$$

This form for the energy shows why the product am of the effective semimajor axis and the mass is slowly varying: In dimensionless units, the energy $\mathcal{E} = -m/2a$ so that

$$(am)^{-1} = -2\mathcal{E}u^2 = E + \mathcal{O}\left(\lambda\right). \tag{70}$$

The product am is thus nearly constant as long as the time scale ratio λ is small, and the departure is of order λ. When λ is small, the orbit cycles through many turning points before the mass changes substantially, so that the average of the above equation becomes

$$\langle (am)^{-1} \rangle = \langle -2\mathcal{E}u^2 \rangle = E + \mathcal{O}\left(\lambda^2\right), \tag{71}$$

so that the average of am is constant to second order.

Number of Cycles: If we ignore J for now and integrate equation (62) over one cycle, we obtain

$$\frac{\gamma\alpha}{E^{1/2}} \int_1^2 \frac{f\,df}{(f - f_1)^{1/2}(f_2 - f)^{1/2}} = \int_1^2 \frac{dx}{x^2} = \frac{1}{x_1} - \frac{1}{x_2}. \tag{72}$$

The integral on the LHS gives us π/E. If we integrate over N cycles we obtain the expression

$$\gamma\alpha N\pi = E^{3/2}\left[1 - m_N^\alpha\right], \tag{73}$$

where we assume that $m = 1$ at the start. The total number of possible cycles occurs when $m_N \to 0$, so that

$$N_T = \frac{E^{3/2}}{\pi\gamma\alpha} = \frac{E^{3/2}}{\pi\gamma(\beta + 1)}. \tag{74}$$

The Last Cycle: The above analysis (if we continue to ignore J) suggests that the last cycle occurs when the right hand side of equation (72) is no longer large enough to balance

the left hand side, which is the same for each cycle. This condition implies that a minimum mass must be left in the star in order for the orbit to complete a cycle (in the function f). This condition can be written in the form

$$m_c = \left(\frac{\pi \gamma \alpha}{E^{3/2}} \right)^{1/\alpha} . \tag{75}$$

Final States: If we set the energy equal to zero and replace the variable x with the time scale ratio λ_f (evaluated at the moment that planet becomes unbound), we find the condition

$$(2f - \eta)^{1/2} = \lambda_f f^{1/2} \pm \left(2f - \eta - Ef^2 - Jf^2 \right)^{1/2} , \tag{76}$$

which can then be written in the form

$$\lambda_f = \frac{(2f - \eta)^{1/2} \pm (2f - \eta - Ef^2 - Jf^2)^{1/2}}{f^{1/2}} . \tag{77}$$

This expression is thus a generalization of that obtained for the special case with $\beta = 0$. The differences are that we have included the extra term J and that the result is written in terms of the variable x instead of u.

The orbital eccentricity, calculated the usual way, oscillates with time with an increasing amplitude of oscillation (e.g., see Figure 4). As shown here, however, the function f executes nearly Keplerian behavior, with nearly constant turning points, where this statement is exact in the limit $J \to 0$. The oscillation of eccentricity, although technically correct, is misleading. The turning points of the orbit (in the original radial variable ξ) are strictly increasing functions of time. The oscillation in e arises because the orbits are not ellipses, and, in part, because the period of the orbits in ξ are not the same as the period of the orbits in f. As a result, the oscillations in the calculated eccentricity do not imply that the near-elliptical shape of the orbit is varying between states of greater and lesser elongation. Instead, these oscillations imply that if the mass loss stops and the orbit once again becomes an ellipse, the value of the final eccentricity of that ellipse oscillates with the ending time of the mass loss epoch.

Final Orbital Elements: Next we consider the case where the planet remains bound after the epoch of stellar mass loss. In this case, we want to estimate the final orbital elements of the planet. Suppose that the orbit passes through N turning points of the function f during the mass loss epoch. The orbit will then complete a partial cycle so that the final value of f lies between the turning points, $f_1 \leq f \leq f_2$. In the ideal case, where we have complete information describing both the starting orbital elements and the final value of the stellar mass, and where the mass loss function is is described exactly by a model with constant
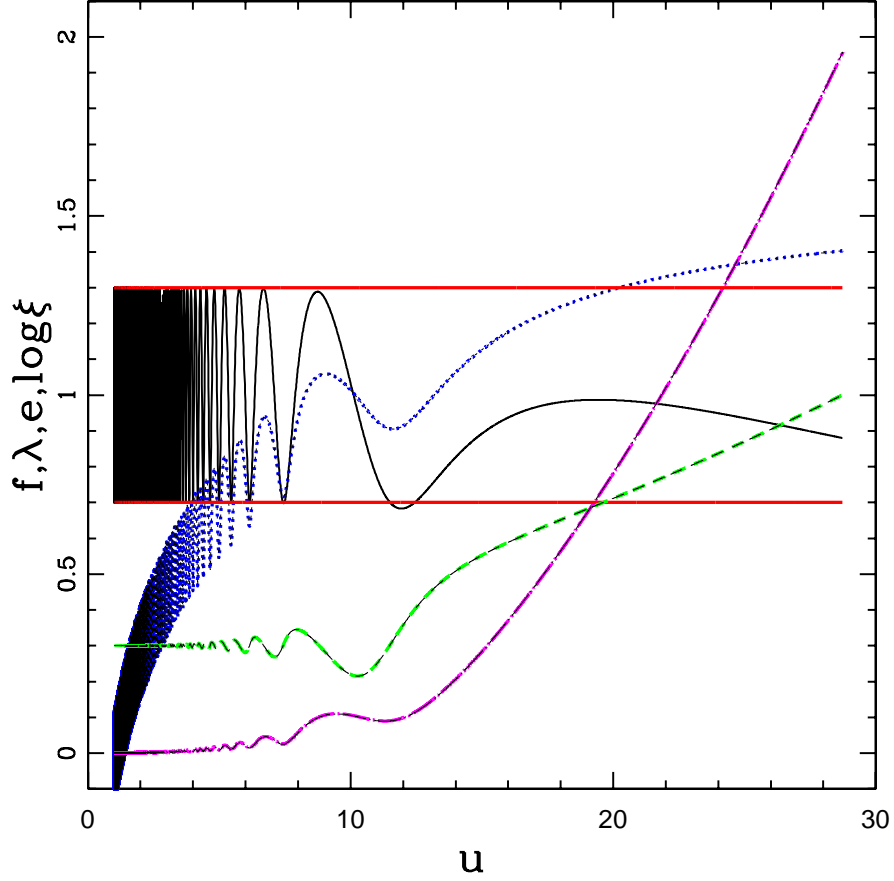
Fig. 3.— Evolution of the orbit during the epoch of stellar mass loss. In this example, the mass loss function has index $\beta = 2$, corresponding to a constant mass loss rate. The other parameters are $\gamma = 10^{-4}$, $e = 0.3$, and $f_0 = 1$ (initially going inward). The black curve shows the function $f(u) = \xi/u$; the red horizontal lines mark the analytically determined turning points of the function. The blue dotted curve shows the evolution of the radial coordinate ξ (plotted here as $\log_{10}[\xi]$). The magenta dot-dashed curve shows the evolution of the time scale ratio λ. Finally, the green dashed curve shows the eccentricity e of the orbit.

index β, we can calculate the final value f_f. In practice, we are likely to have incomplete information. In that case, we can write the average value of the energy in the form

$$2u^2 \mathcal{E} = -E + \frac{\gamma^2 x^2}{E^2} \,, \tag{78}$$

where we have replace f with its effective semimajor axis value $1/E$, and where the remaining term averages to zero. This estimate for the final energy has a uncertainty due to the lack of knowledge of where the planet lies in its orbit during the final cycle. This uncertainty takes the form

$$\frac{\Delta \mathcal{E}}{\mathcal{E}} = \pm \frac{2\gamma x (2f - \eta - Ef^2)^{1/2}}{2u^2 \mathcal{E}} = \pm \frac{2\gamma x e_*}{E^{3/2} - \gamma^2 x^2 / E^{3/2}} \,. \tag{79}$$

With the final energy specified, the final value a_f of the semimajor axis is given by

$$a_f = -\frac{1}{2u\mathcal{E}_f} \,. \tag{80}$$

Similarly, the final value e_f of the orbital eccentricity is given by

$$e_f^2 = 1 + \eta(2u^2 \mathcal{E}_f) = 1 - \eta E + \eta \gamma^2 x^2 / E^2 = e_*^2 + \eta \gamma^2 x^2 / E^2 \,. \tag{81}$$

The expressions derived above for the final orbital elements are expected to be valid provided that the time scale ratio λ is small compared to unity (and hence $|J| \ll 1$). The time evolution of the orbital elements is illustrated in Figure 4 for a representative system with mass loss index $\beta = 2$ and mass loss parameter $\gamma = 10^{-4}$. Numerical integration of the full equation of motion (solid curves) show that the semimajor axis and eccentricity both oscillate and (on average) grow with time. (Note that the Figure plots $\log[a]$.) The values of the elements (a, e) calculated from the average energy (from equation [78]) provide a good approximation to the mean evolution of the orbital elements (see the central dotted curves in Figure 4). Furthermore, using the range of allowed energy calculated from equation (79), we can calculate upper and lower limits to the expected behavior of the semimajor axis and eccentricity (shown as the upper and lower dotted curves). Note that the solutions for a and e oscillate back and forth between these limiting curves. In this example, the planet becomes unbound near $u = 28$. Prior to that epoch, near $u \approx 20$, the bounds on the energy allow for the planet to become unbound, and the upper limit for the semimajor axis approaches infinity. The approximation scheme thus breaks down at this point.

3.5.   Numerical Results for General Mass Loss Indices

The equations of motion can be numerically integrated to find the value ξ_f of the radial coordinate when the system becomes unbound (when the energy becomes positive). For the
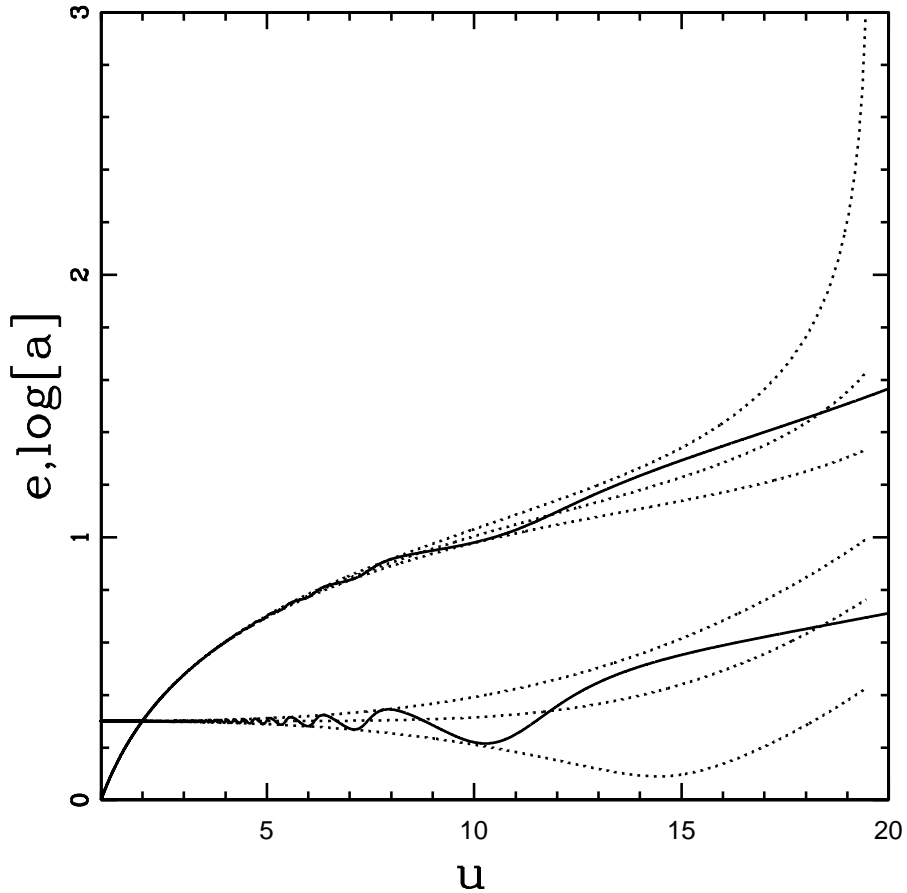
Fig. 4.— Evolution of orbital elements during the epoch of stellar mass loss. In this example, the mass loss function has index $\beta = 2$. The other parameters are $\gamma = 10^{-4}$, $e = 0.3$, and $f_0 = 1$ (initially going inward). The solid curves show the semimajor axis ($\log a$; top) and orbital eccentricity (e; bottom), calculated from numerical integration of the equation of motion. For each orbital element, the three dotted curves show the average value, the upper limit, and the lower limit, as calculated from the analytic expressions given by equations (78 – 81).

case of exponential mass loss, $\beta = 1$, the result is shown in Figure 5 as a function of the mass loss parameter γ (top panel). The figure shows curves for initially circular orbits ($\eta = 1$, smooth curve) and for nonzero starting eccentricity ($\eta = 0.9$, rapidly oscillating curve). The bottom panel shows the value of λ, the ratio of the orbital period to the mass loss time scale, evaluated when the system becomes unbound. As expected, the parameter λ is of order unity when the system energy becomes positive and the planet becomes unbound. For the case of circular orbits at the initial epoch ($\eta = 1$), the value of $\lambda \sim 1.3$ for small γ. For starting orbits with nonzero eccentricity, the value of λ takes on a range of values, but remains of order unity. For the case shown ($\eta = 0.9$, oscillating curve), the parameter λ varies between about $1/2$ and 3.

The above trend holds over a range of values for the mass loss index β. Figure 6 shows the value of the time/mass variable $u = 1/m$ when the planet becomes unbound as a function of the mass loss parameter γ. Results are shown for mass loss indices in the range $-0.5 \leq \beta \leq 3$. For all values of the index β, the curves become nearly straight lines in the log-log plot for small values of γ, which indicates nearly power-law behavior where $u_f \sim \gamma^{-p}$, where the index $p = 1/(\beta + 1)$. A related result in shown in Figure 7, which plots the values of the ratio λ of time scales, evaluated at the moment when the planet becomes unbound, as a function of the mass loss parameter γ. In the limit of small γ, the time scale ratio λ approaches a constant value (of order unity). The finding that λ has a value of order unity (in the limit of small γ) when the planet becomes unbound is expected: In physical terms, this result means that the mass loss time scale has become shorter than the orbital period, so that the potential well provided by the star is changing fast enough that the orbital motion does not average it out.

Nonetheless, the results shown by Figures 6 and 7 are not identical. Suppose that, as shown by Figure 7, $\lambda_f \sim constant$, where the subscript denotes the final value. Since $\lambda = \gamma u_f^{\beta+1} f_f^{3/2} = \gamma u_f^{\beta-1/2} \xi_f^{3/2}$, we infer that $\xi_f \propto \gamma^{-1} u_f^{(2\beta-1)/3}$.

The limiting values of the time scale ratio λ are shown in Figure 8 as a function of the mass loss index β. Here the time scale ratios are evaluated at the moment when the planet becomes unbound. Results are shown for the limiting case of small γ (from Figure 7 we see that the time scale ratio λ approaches a constant values as $\gamma \to 0$). All of the values are of order unity; for the particular case where $\beta = 0$, the final value of the time scale ratio $\lambda = 1$. Since this function $\lambda_f(\beta)$ is useful for analysis of orbits in systems losing mass, we provide a simple fit. If we choose a fitting function of the form

$$\log \lambda_f = a\beta^2 + b\beta, \tag{82}$$

where a and b are constants, we obtain a good fit with the values $a = 0.04102$ and $b = 0.21658$. The fitting function is shown as the dashed curve in Figure 8, and is almost indistinguishable
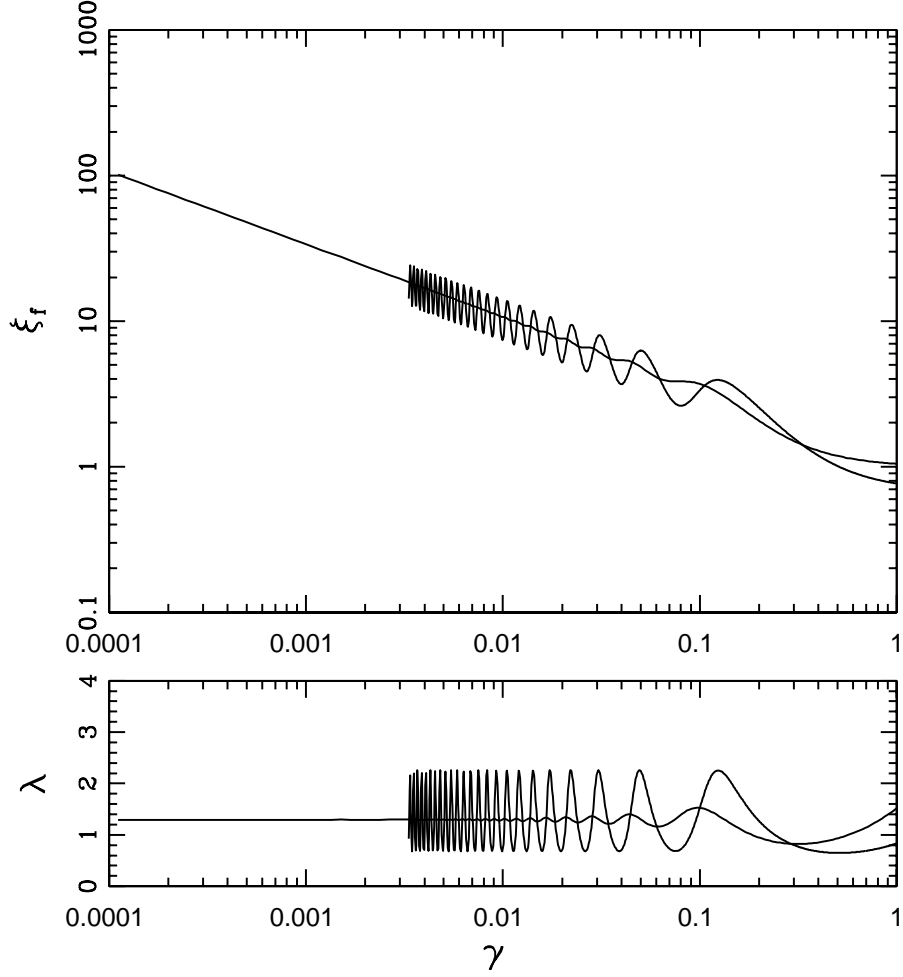
Fig. 5.— Radial coordinate of the planet at the moment when the system becomes unbound, shown here as a function of the mass loss parameter γ for exponential mass loss (top panel). The nearly monotonic curve shows the result for the case of circular starting orbits; the oscillating curve shows the result for angular momentum parameter $\eta = 0.9$ (which corresponds to starting eccentricity $e = \sqrt{0.1} \approx 0.316\ldots$). Bottom panel shows the value of the parameter λ when the planet becomes unbound, for both circular starting orbits (smooth curve) and eccentric orbits ($\eta = 0.9$; oscillating curve). All orbits are started at periastron.
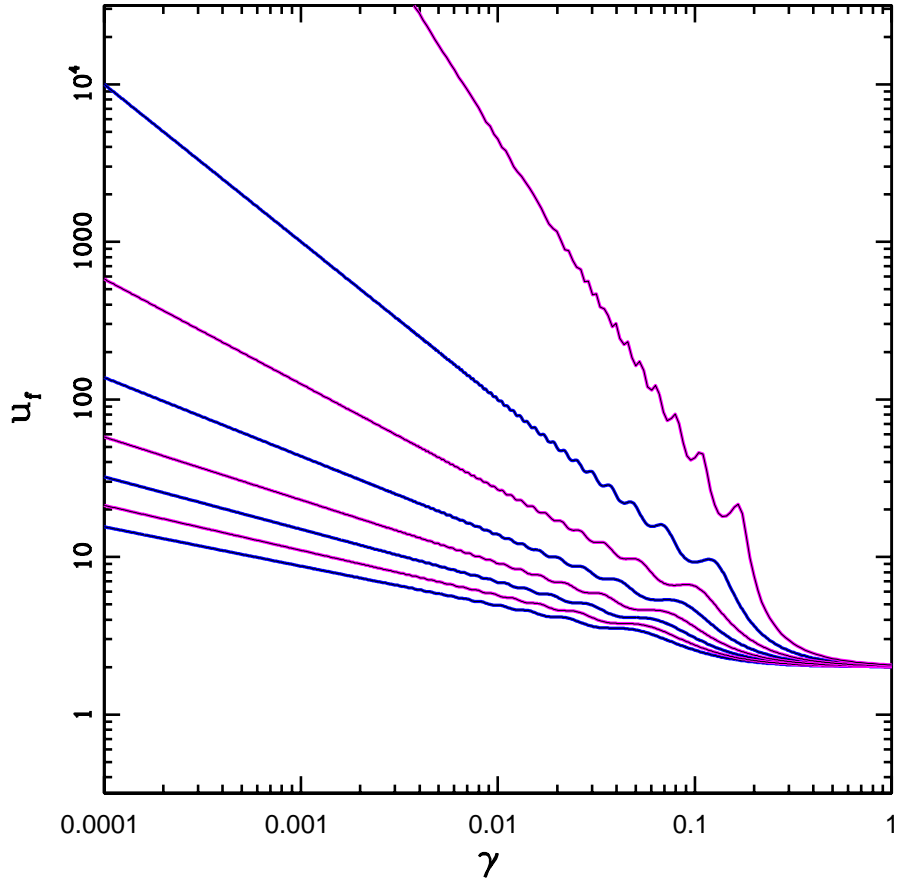
Fig. 6.— Value of the time/mass variable $u = 1/m$ at the moment when the system becomes unbound, shown here as a function of the mass loss parameter γ, for varying values of the index β. All of the curves correspond to circular starting orbits $\eta = 1$ (which corresponds to starting eccentricity $e = 0$). The curves correspond to values of $\beta = -0.5$ (top curve) to 3.0 (bottom curve).
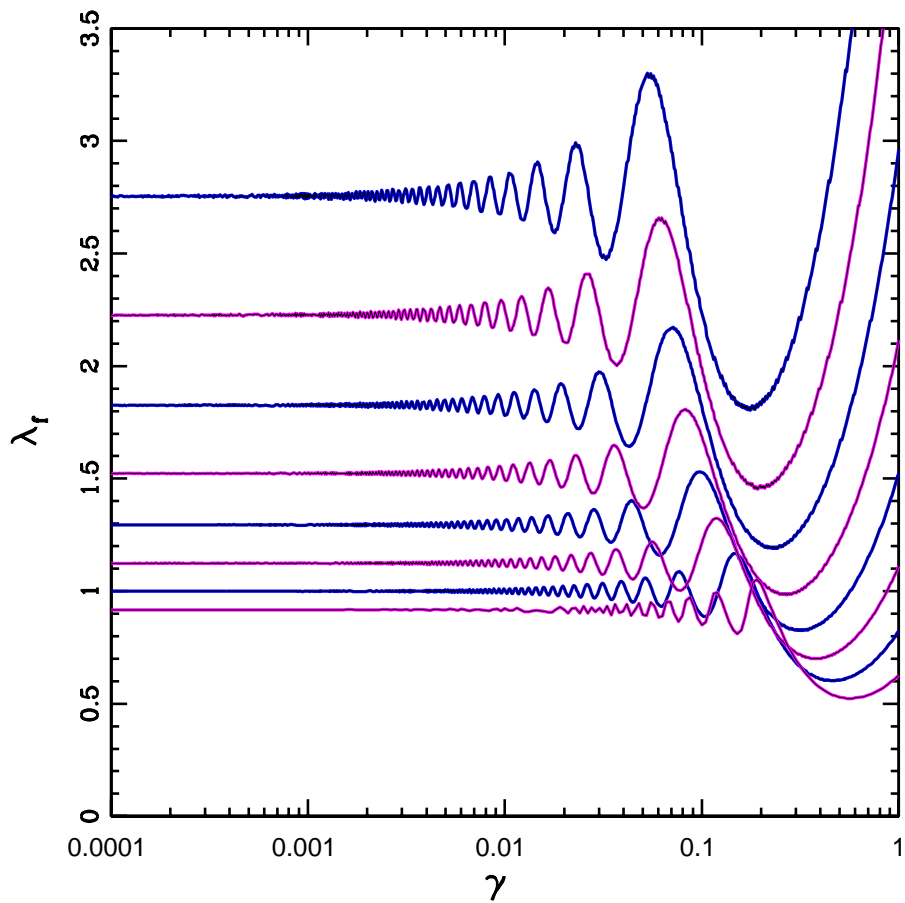
Fig. 7.— Value of the time scale ratio λ evaluated at the moment when the system becomes unbound, shown here as a function of the mass loss parameter γ, for varying values of the index β. All of the curves correspond to circular starting orbits $\eta = 1$ (which corresponds to starting eccentricity $e = 0$). The curves correspond to values of $\beta = -0.5$ (bottom curve) to 3.0 (top curve).

from the numerically integrated solid curve.

4. Lyapunov Exponents for Two Planet Systems with Mass Loss

The remainder of this paper focuses on the particular case $N = 3$, i.e., a system consisting of two planets and a central star. To first approximation, such a configuration is a relatively good model for our own solar system, where the motion of only the three most dominant bodies (Jupiter, Saturn and the Sun) are considered. For this paper, we fix the planetary masses and initial orbital elements to those of Jupiter and Saturn, and the initial star mass to $M_* = 1 M_\odot$. We also restrict the orbits to a plane, thereby reducing the number of phase space variables from 18 to 12.

As long as the planets suffer no close encounters, the general dynamics for each planet are similar to the dynamics of the variable mass two-body problem. An example of the osculating orbital elements (a, e) of a typical system is shown in Figure 9. As each planet orbits in an outward spiral, the semimajor axis increases approximately exponentially. The eccentricity oscillates rapidly on orbital timescales, and more slowly on secular timescales (as the planets exchange angular momentum) but remains approximately constant up until roughly a few e-folding times for the stellar mass loss. The product of the semimajor axis and star mass $(a M_*)$ is also approximately constant until a few e-folding times have past. At this point, the orbital elements $a \to \infty$ and $e \to 1$ and planets can become unbound. Notice that at this point, the stellar mass is only a few percent of the initial value and thus, this scenario is rather artificial for stars like our Sun, which are only expected to lose about half of their initial masses. However, larger stars lose a greater fraction of their original masses. For example, a star with initial mass $M_* \approx 8 M_\odot$ must end its life as a white dwarf with less than $\sim 15\%$ of its original mass.

The evolution of the orbital elements can differ dramatically if the planets reach a small enough separation so that orbital crossings can occur. In this regime, chaos dominates and the orbital elements evolve in a less predictable manner. An example is shown in Figure 10 for the same parameters as Figure 9 but with the initial eccentricity of the inner planet (Jupiter) increased to $e = 0.3$. Although the system initially exhibits somewhat periodic behavior, by the time $t = \tau$ this stability has been disturbed.

Traditionally, studies of dynamical systems have used the maximum Lyapunov exponent as an indication of the level of chaos present (e.g., Lichtenberg & Lieberman 1983; Strogatz 1994). If a system is chaotic, two nearby trajectories in phase space differing by a small
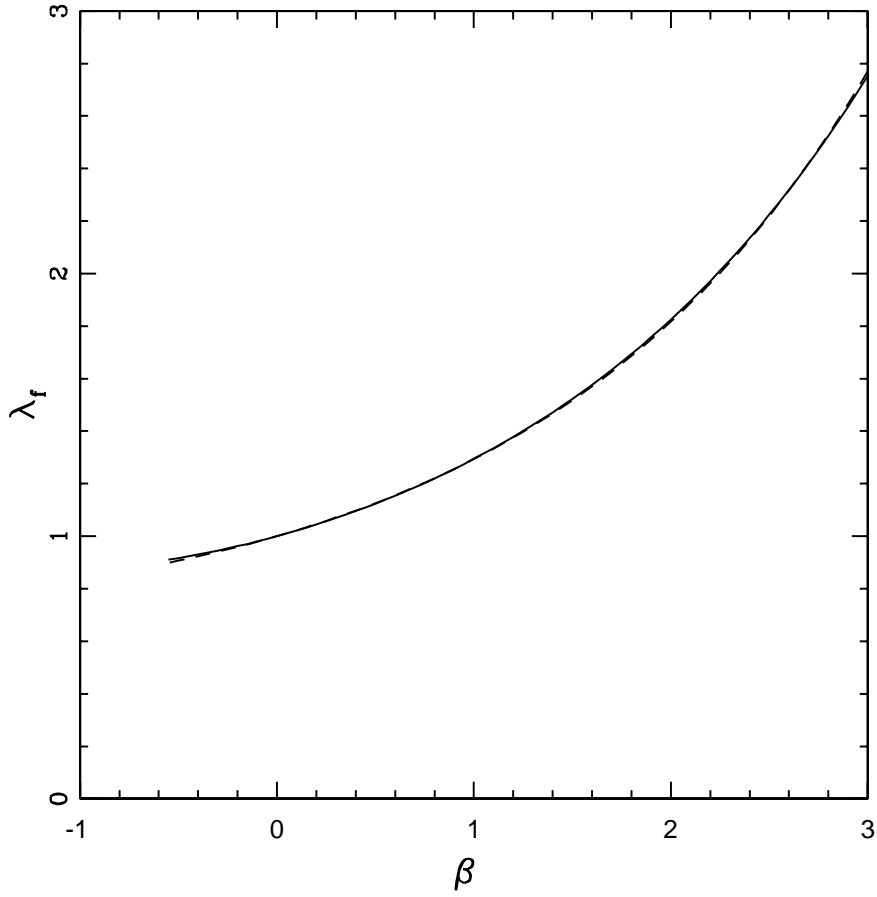
Fig. 8.— Value of the time scale ratio λ evaluated at the moment when the system becomes unbound, shown here as a function of the mass loss index β which defines the time dependence of stellar mass loss. These values correspond to the limit of small mass loss parameter $\gamma \to 0$ and the limiting case where the eccentricity of the starting orbit $e = 0$. The dashed curve, which is nearly identical to the solid curve, shows a simple fit to the function $\lambda_f(\beta)$, as described in the text. As shown in the text, $\lambda_f = 1$ for the particular case $\beta = 0$.
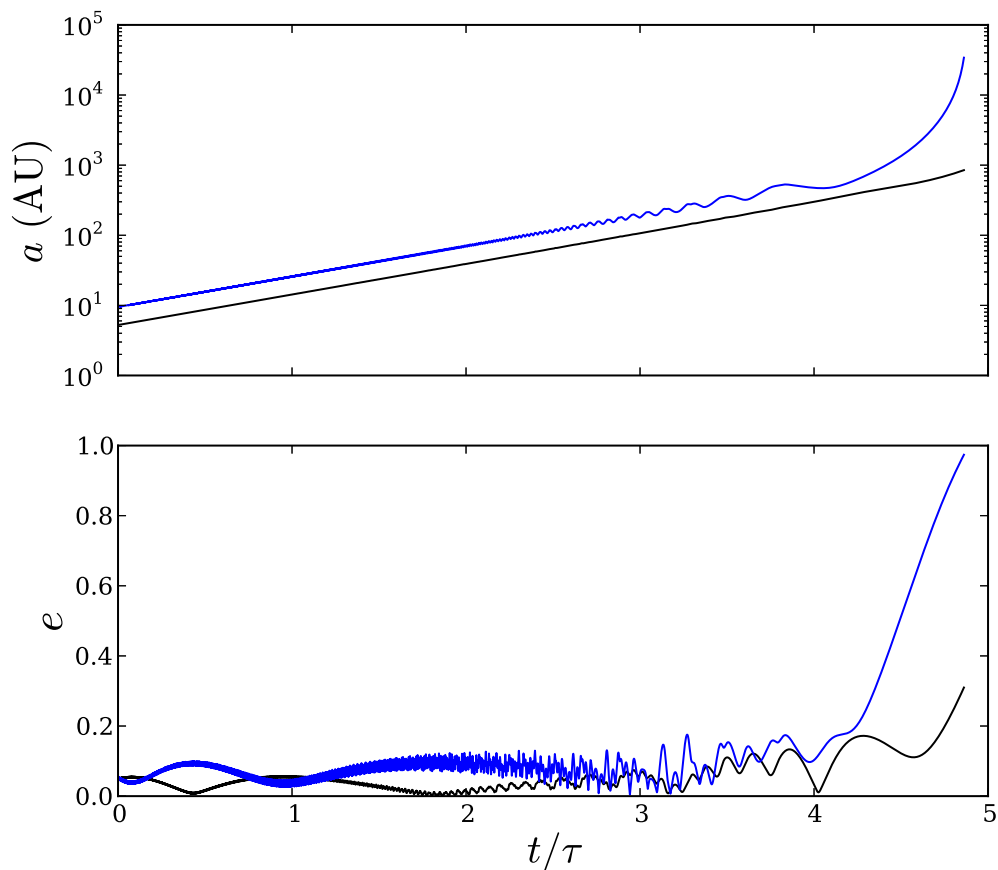
Fig. 9.— Osculating semimajor axis and orbital eccentricity for a pair of planets orbiting an initially solar-mass star with mass loss timescale $\tau = 10^5$ years. Planets have masses, initial semimajor axis and eccentricities of Jupiter and Saturn. The orbital elements evolve in a roughly predictable manner, with the semimajor axes increasing smoothly and the eccentricities oscillating on secular timescales, but remaining relatively constant until the star has lost the majority of its initial mass.
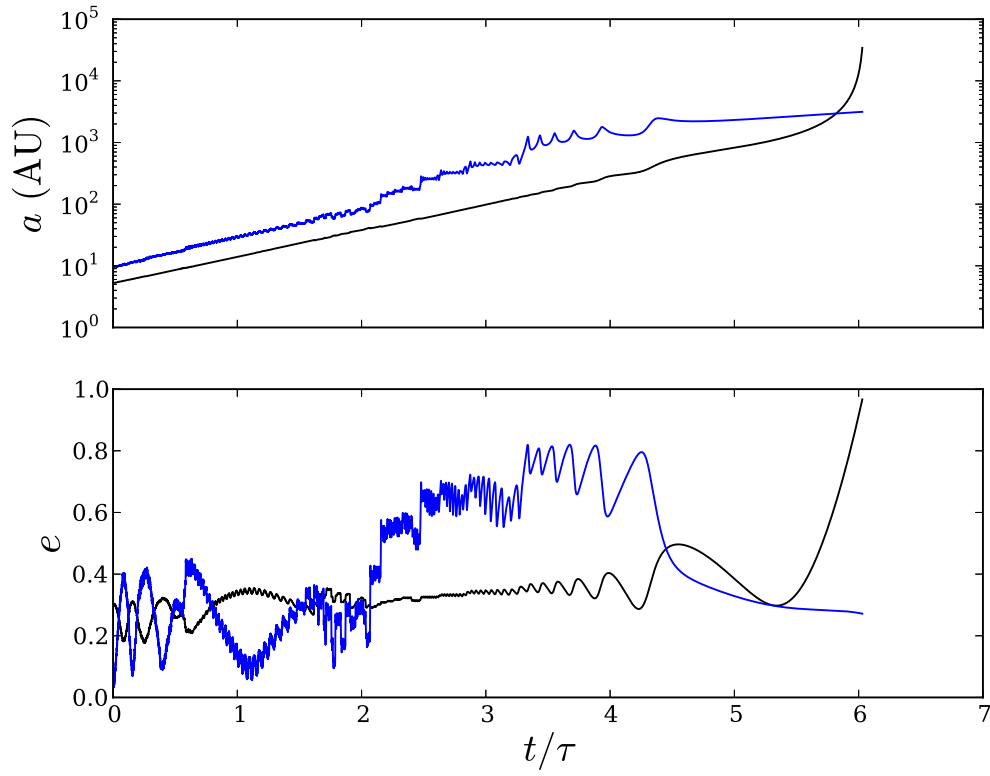
Fig. 10.— Same as Figure 9, but with the initial eccentricity of Jupiter increased to $e_0 = 0.3$. This increase in eccentricity allows for orbital crossings and increases chaotic behavior.

amount δ_0 should diverge according to

$$\delta(t) = \delta_0 e^{\Lambda t} \qquad \text{with} \qquad \Lambda > 0. \tag{83}$$

The Lyapunov time is thus $\tau = 1/\Lambda$. The long-term dynamical stability of the solar system has been explored in the absence of stellar evolution (Batygin & Laughlin 2008; Laskar 2008), and current estimates of the Lyapunov time for the solar system (while the mass of the Sun remains constant) are $\tau \approx 5$ Myr (Sussman & Wisdom 1992), but this number decreases when stellar mass loss is introduced, as demonstrated below.

Here we determine the Lyapunov times as a function of the mass loss timescale via numerical integrations. We define a "real" system along with a "shadow" system where the initial conditions of the shadow system differ by a small amount δ_0. By integrating both systems simultaneously and monitoring the quantity $\delta(t)$ (i.e., the level of divergence of the neighboring trajectories), the maximum Lyapunov exponent can be extracted. Since a three-body system restricted to a plane consists of 12 phase space variables, there is some choice in defining the quantity δ. We define δ such that

$$\delta = \sqrt{(x_r - x_s)^2 + (y_r - y_s)^2}, \tag{84}$$

where the subscripts r and s refer to the "real" and "shadow" trajectories respectively. Figure 11 shows an example of $\ln \delta$ versus time for different values of the mass loss timescale τ. After an initial period of transient growth (roughly delimited by $t \gtrsim 0.3\tau$), the divergence metric $\delta(t)$ increases exponentially with time and the Lyapunov exponent can be obtained by finding the slope of the line defined by $\ln \delta = \ln \delta_0 + \Lambda t$.

For each value of the mass loss timescale τ, the maximum Lyapunov exponent was calculated. Since the maximum possible separation between the reference and shadow systems is finite (using the definition of δ in equation [84]), the curves of growth eventually saturate. Thus, to extract the Lyapunov exponent Λ, we want to choose portions of the curves of divergence following the initial transient behavior but before saturation occurs. In most cases, Λ was calculated from the time-series data for times $\tau/3 \leq t \leq \tau$ (the regions between the vertical dashed lines in Figure 11). An exception was made for very slow mass loss however, where $\tau = 100$ Myr. In such scenarios, the timescale for mass loss is greater than the "natural" Lyapunov time of ~ 10 Myr (without mass loss), and the curves of divergence saturate before $t = 0.3\tau$. In this case, Λ was calculated only for time series data $t < 10$ Myr.

Figure 12 shows our numerical values of the Lyapunov times τ_{ly} as a function of the mass loss time τ_{m}. We performed the analysis described above for each of the two planets in the system separately and averaged the results. The horizontal dotted line–included here mainly for reference–is our numerical value of the Lyapunov time for the solar system without

mass loss. Our value is in relatively good agreement with previous calculations (Sussman & Wisdom 1992), but differs slightly because our model considers only two of the four giant planets. As $\tau_\mathrm{m} \to \infty$, the Lyapunov time approaches the dotted line. The squares show the values of τ_m where points were actually calculated, and the dashed line indicates the least-squares fit (for $\tau_\mathrm{m} \leq 10^7$ only). It is interesting to notice that the slope of this line is almost exactly unity. In other words, we obtained

$$\tau_\mathrm{ly} \sim \tau_\mathrm{m}^p \qquad \text{where} \qquad p = 0.992. \tag{85}$$

Note that this line cannot be extrapolated below $\tau_\mathrm{m} = 10^2 - 10^3$; in this regime, τ_m is comparable to the orbital timescales of the planets, and the mass loss cannot be considered adiabatic. As a result, the dynamics will differ considerably.

As a consistency check, we also explored other choices for δ. An especially compelling option is to use the semimajor axis a, because unlike the physical distance between the reference and shadow trajectories, there is no upper limit on this quantity. The previous calculation was thus repeated using

$$\delta = |a_r - a_s|. \tag{86}$$

Our results are quite similar however, which indicates that the Lyapunov times do not depend sensitively on the choice of δ.

We want to ensure that the (nearly) linear relation between the Lyapunov time and mass loss time is not an artifact of the exponential ($\beta = 1$) mass loss law that was chosen. Toward this end, we have explored two additional functional forms for the mass loss law: The first used vanishing mass loss index $\beta = 0$ (see equation [21]), whereas the second used a constant mass loss rate with $\beta = 2$ (see equation [19]). For both of these mass loss function, we obtained the same power-law relations for these mass loss forms ($\tau_\mathrm{ly} \sim \tau_\mathrm{m}^p$), where $p = 0.981$ and $p = 1.012$ using equations (21) and (19), respectively. The results, shown in Figure 13, are thus nearly identical, regardless of the mass loss law, which suggests that this power-law trend is robust.

5. Conclusion

This paper has reexamined the classic problem of the evolution of planetary orbits in the presence of stellar mass loss. Although this issue has been addressed in previous studies (see the discussion of Section 1), we generalize existing work to include a wider class of time dependence for the mass loss function and to determine Lyapunov time scales for multiple planet systems. Our main results can be summarized as follows:
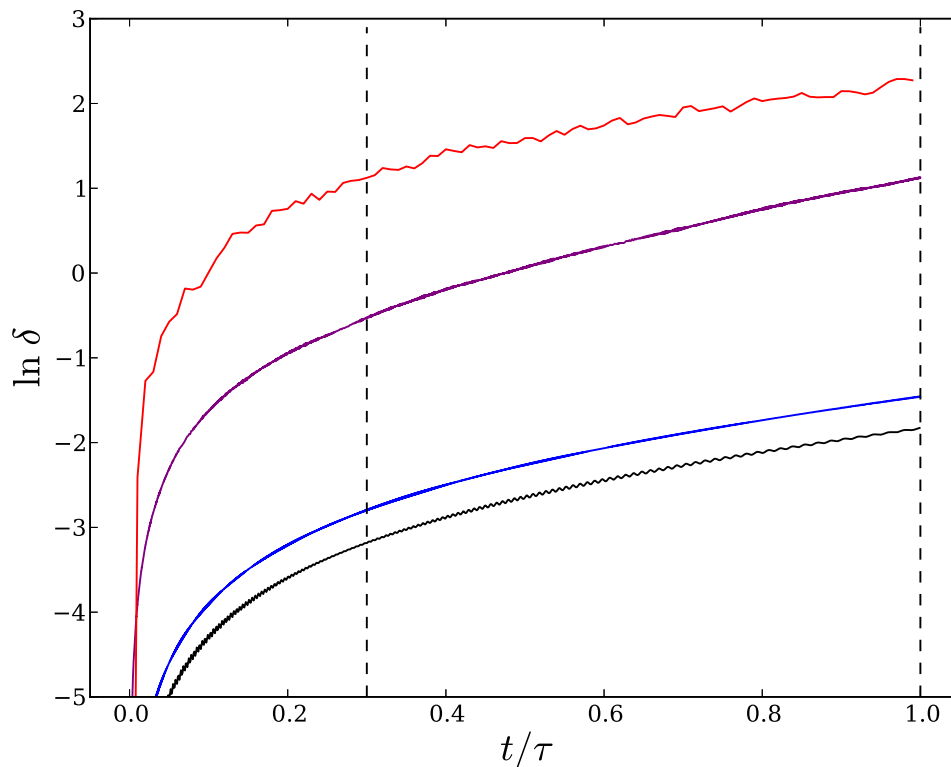
Fig. 11.— Curves showing the divergence of two trajectories separated by a small distance δ_0 for different values of the mass loss timescale τ. Black curve is $\tau = 10^4$; blue is $\tau = 10^5$; purple is $\tau = 10^6$; and red is $\tau = 10^7$ (yr). After a period of initial growth, the trajectories diverge exponentially, indicated by the linear shape of the latter portions of the graphs. The regions between the dashed lines were used to calculate the Lyapunov exponent. Note that the time variable has been scaled by the mass loss timescale τ.
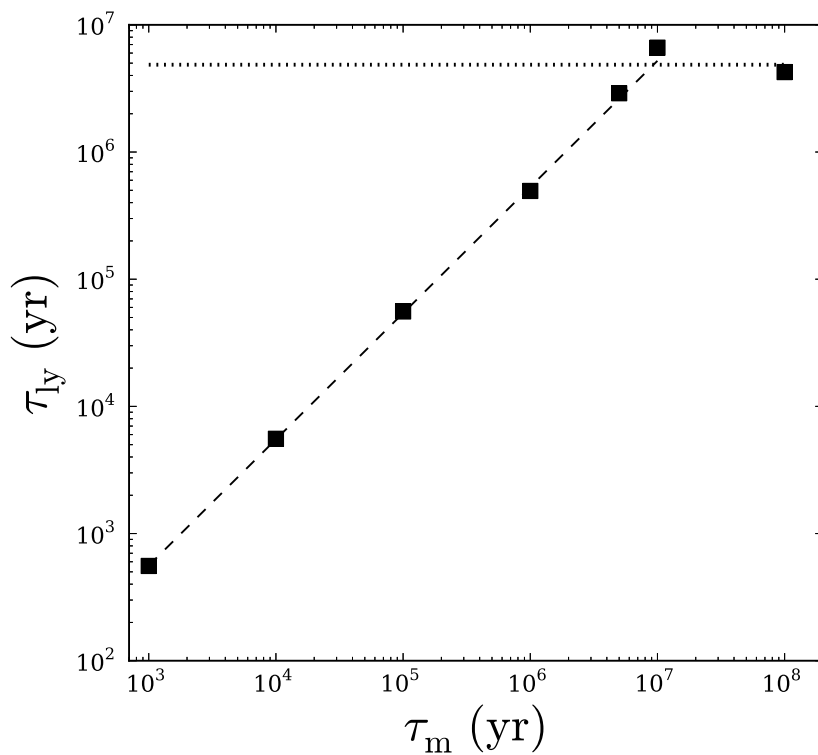
Fig. 12.— Calculated Lyapunov times τ_{ly} versus mass loss timescales τ_{m} for a star losing mass exponentially (mass loss index $\beta = 1$). The calculated quantities are shown (square symbols) along with their least-squares fit for $\tau_{\mathrm{m}} \leq 10^7$ (dashed line). As $\tau_{\mathrm{m}} \to \infty$, the Lyapunov time approaches that of the solar system with constant stellar mass (~ 5 Myr, as marked by the horizontal dotted line).
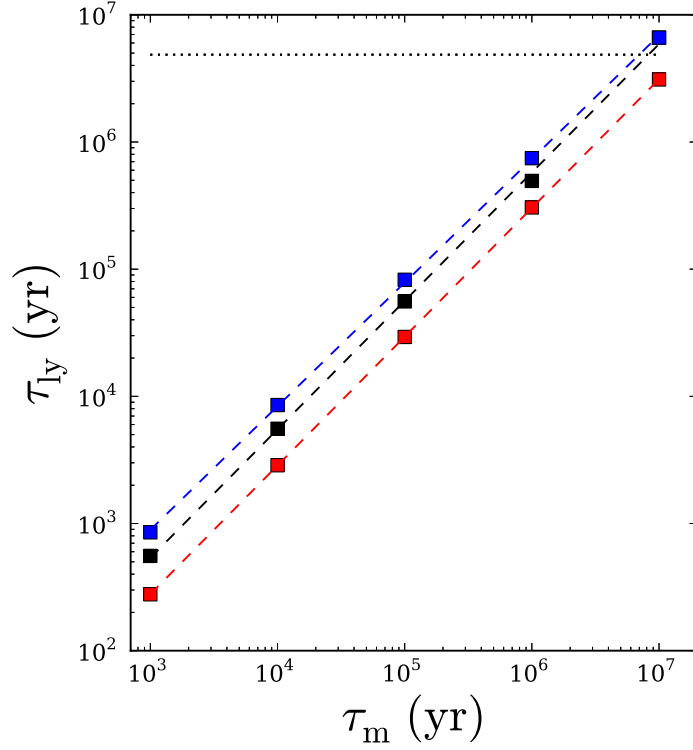
Fig. 13.— Lyapunov timescale τ_{ly} versus mass loss timescale τ_m for systems where the star loses mass through three different decay laws. Black curve shows the results for exponential mass loss ($\beta = 1$); the blue curve shows the results for $\beta = 0$; the red curve shows the results for constant mass loss rate ($\beta = 3$). The similar structure of all three of the lines indicate that the results are largely independent of the particular mass loss formula.

[1] This paper presents an alternate formulation of the classic problem of orbits with stellar mass loss. The resulting equations of motion are valid for the case where the mass loss index β is constant (see equation [10]), which allows for a wide range of time dependence of the mass loss rates. Previous numerical studies show that planetary orbits often obey the approximate law $am \approx constant$, where a is the semimajor axis of the orbits, and where this approximation holds as long as the mass loss time scale is significantly longer than the orbital period. By writing the equation of motion in the form given by (24) and (25), we show analytically why this law holds. For completeness, we note that the orbits retain a nearly constant eccentricity during this phase of evolution, so that the semimajor axis increases nearly monotonically while the orbital radius ξ oscillates in and out.

[2] In the limit of rapid mass loss, $\lambda \to \infty$, we obtain analytic solutions that describe orbits for the entire class of mass loss functions (see Section 3.3). The condition for the planet becoming unbound is given by equation (52). For planets that remain bound, the new orbital elements are given by equation (58).

[3] Not all mass loss functions lead to planets becoming unbound (except, of course, in the extreme case where the stellar mass vanishes $m \to 0$). The critical value of the mass loss index is $\beta = -1$, where systems with mass loss characterized by $\beta < -1$ only lose planets in the $m \to 0$ limit. Note that systems with the transition value of the mass loss index $\beta = -1$ were first considered by Jeans (1924).

[4] For the particular, intermediate value of the mass loss index $\beta = 0$, we can find analytic expressions for the function $f(u)$ and for the final values of the time scale ratio λ_f when the planet becomes unbound (see Section 3.2).

[5] One way to characterize the dynamics of these systems is through the parameter λ_f. We define λ to be the square of the ratio of dimensionless mass loss rate to the orbital frequency, and λ_f is the value at the moment when the planet becomes unbound. For initially circular orbits, the parameter λ_f is always of order unity, and approaches a constant value in the limit of small mass loss rates γ; further, the value of this constant varies slowly with varying β (see Figure 7). For orbits starting with nonzero eccentricity, however, the parameter λ_f can depart substantially from unity and varies significantly with β (compare Figures 1 and 2).

[6] For multiple planet systems, we find that the Lyapunov times decrease in the presence of stellar mass loss, so that chaos should play a larger role in planetary dynamics as stars leave the main sequence. For a typical mass loss timescale of $\tau_{\rm m} \sim 10^6$ yr, the Lyapunov time is reduced by nearly a factor of ten. Three different functional forms for the stellar mass loss have been considered, all yielding similar results, which suggests that our results

are robust.

There are many opportunities for future work. This paper has focused on our own solar system, and has considered only the motion of Jupiter, Saturn, and the Sun, since these are the most gravitationally dominant bodies. However, future calculations should also include Uranus and Neptune. Additionally, this paper has considered relatively short integrations, spanning at most only $10 - 100$ Myr. Although stellar mass loss is not expected to continue for longer than 100 Myr, the increased semimajor axes of the planets will change the overall dynamics and the decreased stellar mass (relative to the planets) could lead to an increase in dynamical instabilities. Thus, longer integrations should be performed, using the lower (constant) stellar mass and the increased semimajor axes of the planets as input. Finally, given the diversity exhibited in the observed sample of extrasolar planets, different planetary configurations should also be considered. These types of calculations will help us understand the long term fate of planetary systems in general and help direct future observations.

A. Bounds on the Integral J

In the limit $|J| \ll 1$, we have a completely analytic description of the dynamics. It is thus useful to place bounds on the integral J, which can be done as follows: First write

$$J = \gamma^2 \beta I \qquad \text{where} \qquad I = 2 \int_1^x x^2 f f_x dx \,. \tag{A1}$$

Note that since the function f is of order unity, the order of J is given by

$$J = \mathcal{O}\left(\gamma^2 x^2\right) = \mathcal{O}\left(\lambda^2\right) \,. \tag{A2}$$

Next we integrate by parts to obtain

$$I = x^2 f^2 - f_0^2 - 2 \int_1^x x f^2 dx \,. \tag{A3}$$

The second integral can be written

$$2 \int_1^x x f^2 dx = 2\langle f^2 \rangle \int_1^x x dx = \langle f^2 \rangle (x^2 - 1) \,, \tag{A4}$$

where we have invoked the mean value theorem. The function f varies between turning points so that $f_1 \leq f \leq f_2$. We thus have bounds

$$I \leq x^2(f_2^2 - f_1^2) + f_1^2 - f_0^2 \leq x^2(f_2^2 - f_1^2), \tag{A5}$$

and

$$I \geq x^2(f_1^2 - f_2^2) + f_2^2 - f_0^2 \geq x^2(f_1^2 - f_2^2). \tag{A6}$$

As a result, we have the bound

$$|I| \leq x^2(f_2^2 - f_1^2) = x^2(f_2 + f_1)(f_2 - f_1) = x^2 4 a_*^2 e_* . \tag{A7}$$

We thus obtain the desired bound on J, i.e.,

$$|J| \leq \beta \gamma^2 x^2 (f_2 + f_1)(f_2 - f_1) = \gamma^2 x^2 4 \beta a_*^2 e_* . \tag{A8}$$

In order to evaluate this bound, we need expressions for the turning points f_1 and f_2, or, equivalently, the effective semimajor axis a_* and eccentricity e_*. As derived in the text, we have approximations for these quantities, where these expressions are exact in the limit $J \to 0$.

REFERENCES

Abramowitz, M., & Stegun, I. A., 1970, Handbook of Mathematical Functions (New York: Dover)

Adams, F. C., & Laughlin, G. 1997, Rev. Mod. Phys., 69, 337

Batygin, K., & Laughlin, G. 2008, ApJ, 683, 1207

Bear, E., & Soker, N. 2011, MNRAS, 414, 1788

Debes, J. H., & Sigurdsson, S. 2002, ApJ, 572, 556

Diacu, F., & Selaru, D. 1998, J. Math. Phys., 39, 6537

Duff, M. J., Okun, L. B., & Veneziano, G. 2002, JHEP, 0203, 023

Duncan, M. J., & Lissauer, J. J. 1998, Icarus, 134, 303

Hadjidemetriou, J. D. 1963 Icarus, 2, 440

Hadjidemetriou, J. D. 1966 Icarus, 5, 34

Hurley, J. R., Pols, O. R., & Tout, C. A. 2000, MNRAS, 315, 543

Jeans, J. H. 1924, MNRAS, 85, 2

Jura, M., 2003, ApJ, 584, L91

Kratter, K. M., & Perets, H. B. 2012, ApJ, 753, 91

Kudritzki, R. P., & Reimers, D. 1978, A&A, 70, 227

Laughlin, G., & Adams, F. C. 2000, Icarus, 145, 614

Laskar, J. 2008, Icarus, 196, 1

Lichtenberg, A. J., & Lieberman, M. A. 1983, Regular and Chaotic Dynamics (Springer-Verlag, New York)

Melis, C., Jura, M., Albert, L., Klein, B., & Zuckerman, B. 2010, ApJ, 722, 1078

Moeckel, N., & Veras, D. 2012, MNRAS, 422, 831

Murray, C. D., & Dermott, S. F. 1999, Solar System Dynamics (Princeton: Princeton Univ. Press)

Mustill, A. J., & Villaver, E. 2012, ApJ, in press, arXiv:1210.0328

Perets, H. B., & Kratter, K. M. 2012, arXiv:1203.2914

Schröder, K.-P., & Connon Smith, R. 2008, MNRAS, 386, 155

Spiegel, D. S., & Madhusudhan, N. 2012, ApJ, 756, 132

Strogatz, S. H. 1994, Nonlinear Dynamics and Chaos (Addison-Wesley, MA)

Sussman, G. J., & Wisdom, J. 1992, Science, 257, 56

Uzan, J.-P. 2003, Rev. Mod. Phys., 75, 403

Veras, D., Wyatt, M. C., Mustill, A. J., Bonsor, A., & Eldridge, J. J. 2011, MNRAS, 417, 2104

Veras, D., & Tout, C. A. 2012, MNRAS, 422, 1648

Veras, D., & Wyatt, M. C. 2012, MNRAS, 421, 2969

Villaver, E., & Livio, M. 2007, ApJ, 661, 1192

Villaver, E., & Livio, M. 2009, ApJ, 705, 81

Vinti, J. P. 1974, MNRAS, 169, 417

Wolszczan, A. 1994, Science, 264, 538

Zuckerman, B., Melis, C., Klein, B., Koester, D., & Jura, M. 2010, ApJ, 722, 725